AUTOMATED FITTING OF THERMOGRAVIMETRIC ANALYSIS DATA

Morgan C. Bruns [A] and Isaac T. Leventon [B]
[A] *Virginia Military Institute, Department of Mechanical Engineering*
710 Nichols Hall; Lexington, VA 24450; United States

[B] *National Institute of Standards and Technology, Fire Research Division,*
100 Bureau Drive; Building 224, Room A265; Gaithersburg, MD 20899; United States

ABSTRACT

A novel methodology has been developed for extracting pyrolysis kinetic parameters from thermogravimetric analysis (TGA) data. The development of this methodology is motivated by a need to automate the determination of material properties for use in fire models. The algorithm with which the methodology is implemented is described. Aside from being fully-automated, the resultant script has the advantage of being efficient—a full set of kinetic parameters is provided in less than one second. The script is verified against manufactured TGA data for one and two reaction mechanisms and the effects of reaction peak width and the distance between reaction peaks is examined. Validation is accomplished by applying the script to TGA data for Nylon 6,6, a flexible polyurethane (PU) foam, and polyvinyl chloride (PVC). The resultant kinetic parameters are tabulated, and plots of the actual and predicted TGA data show that the algorithm is quite effective for one, two, and three reaction mechanisms.

INTRODUCTION

Computational fire models have proven to be effective at predicting the spread of heat and smoke in a wide range of building fire scenarios. However, such models still generally require user input describing the actual fire that is generating the heat and smoke. Computational predictions of flame spread and fire growth require somewhat detailed models of condensed phase physics, and a number of condensed phase pyrolysis models have been developed[1-3]. Such models have proven effective at modeling the burning rate of small slabs, but their application to flame spread calculations is more limited. Part of the problem is that these pyrolysis models require the specification of a large number of material properties. Furthermore, there are many different flammable materials that need to be considered in fire scenarios. Substantial progress in applying computational fire models to predicting flame spread could be achieved by the development of both a streamlined methodology for characterizing the thermophysical properties of flammable materials as well as the creation of a publicly available database of such material properties.

One successful approach for characterizing materials is based on performing a number of milligram-scale and bench scale tests such as thermogravimetric analysis (TGA), differential scanning calorimetry (DSC), and the controlled atmosphere pyrolysis apparatus (CAPA)[4]. An example of a public database of material properties is found in the Validation Guide of the Fire Dynamics Simulator (FDS)[5]. Currently, an international effort is underway to further develop experimental and modeling tools such as these in order to "advance predictive fire modelling"[6]. The present manuscript presents work based on a coordinated effort to develop a comprehensive database of material properties for use in fire models. This database will include both raw data from a suite of milligram-scale tests and a list of properties for each material that could be directly used as inputs for a fire model such as FDS. In order to generate these tables of material properties, automated computational scripts are required to robustly analyze raw data from small scale tests. In this paper, we present such a script for calibrating a generalized pyrolysis kinetic model to TGA data. Previous work has looked

at optimization algorithms[7] and Markov Chain Monte Carlo (MCMC) methods[8] for fitting TGA data, but these approaches are not fully automated for general multi-step reaction schemes and can be relatively computationally expensive.

THEORY

In thermogravimetric analysis (TGA), the mass of a small sample of material is measured while heated according to a prescribed temperature program. Typically, the sample will be heated at a constant temperature ramp rate. If the sample mass and heating rate are sufficiently small, then the temperature and composition throughout the sample are approximately uniform. As the material is heated, chemical bonds are broken producing smaller molecules. Eventually, the products of pyrolysis become small enough to vaporize, and mass is lost from the system. Models of this process typically take the form of a system of reactions with unimolecular Arrhenius kinetics.

Independent Unimolecular Reactions

In the following, focus is limited to systems of independent reactions. This generalized model could account for (1) a system of parallel reactions or (2) a system of series reactions in which the subsequent reactions occur at different temperatures. To begin, consider a system of N_r unimolecular reactions of the form

$$\mathrm{R}_i \xrightarrow{k_i} \nu_i \mathrm{C} + (1-\nu_\mathrm{i})\mathrm{G}, \quad i = 1, \ldots, N_\mathrm{r} \tag{1}$$

where R_i is the label for the reactant material, C is the label for the condensed phase products of the reaction, k_i is the reaction rate constant, ν_i is the residual mass fraction of the reaction, and G is the label for the gas species which escapes the sample. For the purposes of the following analysis, it is not necessary to distinguish between the condensed phase and gas phase products of the reactions. Additionally, consideration will be limited to constant heating rate TGA experiments in which the sample temperature increases at a constant rate, β. An Arrhenius model is assumed for the temperature dependence of the rate constant such that, for each reaction

$$k_i = \left(\frac{A_i}{\beta}\right) \exp\left(-\frac{E_i}{RT}\right) \tag{2}$$

where A_i is the pre-exponential, E_i is the activation energy, and R is the gas constant. Note that the heating rate has been directly absorbed into the rate constant in order to simplify the notation in the following analysis. Consequently, k_i is not strictly speaking the Arrhenius rate constant, but the kinetic pair (A_i, E_i) are the true Arrhenius pre-exponential and activation energy, respectively.

For the kinetic model described by Eqs. [1], the temperature rate of change of the mass of component i, m_i, is governed by

$$m_i' \equiv \frac{\mathrm{d}m_i}{\mathrm{d}T} = -m_i k_i \tag{3}$$

along with the initial condition $m_i(T_0) = m_{0,i}$ where T_0 is the initial temperature of the TGA experiment (or any temperature prior to the onset of the reaction). The total sample mass of the sample is simply the sum of the individual component masses. The total mass loss rate must account for the generation of residual solid products of the reactions so that

$$m' \equiv \frac{\mathrm{d}m}{\mathrm{d}T} = \sum\nolimits_i (1-\nu_i) m_i' \tag{4}$$

Non-Dimensional Form and Approximate Solution

It is convenient to non-dimensionalize Eq. [3], and the resultant non-dimensionalization leads to an approximate solution which is valid for most materials. The peak mass loss rate may be found by differentiating Eq. [3] with respect to temperature and setting the result equal to zero. Analysis of this peak condition yields the following results. Using $T_{\mathrm{p},i}$, $m_{\mathrm{p},i}$, and $m'_{\mathrm{p},i}$ to denote the temperature, mass, and temperature derivative of the mass corresponding to that peak, a characteristic width of the peak may be defined as

$$\Delta T_i \equiv \frac{-m_{\mathrm{p},i}}{m'_{\mathrm{p},i}} = \frac{RT_{\mathrm{p},i}^2}{E_i} \qquad [5]$$

where the second equality in Eq. [5] is determined from analysis of the peak equation. The kinetic equations can be recast in terms of the peak temperature and the peak width parameters which are related to the Arrhenius parameters through

$$E_i = \frac{RT_{\mathrm{p},i}^2}{\Delta T_i} \qquad [6]$$

$$A_i = \frac{\beta}{\Delta T_i} \exp\left(\frac{T_{\mathrm{p},i}}{\Delta T_i}\right) \qquad [7]$$

A simplified form of the kinetic equations may be obtained using the following non-dimensionalization

$$\mu_i \equiv \frac{m_i}{m_{0,i}} \qquad [8]$$

$$\theta_i \equiv \frac{T - T_{\mathrm{p},i}}{\Delta T_i} \qquad [9]$$

The non-dimensional kinetic equation for component i becomes

$$\mu'_i \equiv \frac{\mathrm{d}\mu_i}{\mathrm{d}\theta_i} = -\mu_i \exp\left(\frac{\theta_i}{\xi_i \theta_i + 1}\right) \qquad [10]$$

with the boundary condition $\mu_i(\theta_i \to -\infty) = 1$ where $\xi_i \equiv \Delta T_i / T_{\mathrm{p},i}$ may be thought of as a shape parameter for the mass loss peak.

For the limiting case in which $\xi_i \to 0$, Eq. [10] has the exact solution

$$\mu_i = \exp[-\exp(\theta_i)] \qquad [11]$$

or, in dimensional form,

$$m_i = m_{0,i} \exp\left[-\exp\left(\frac{T - T_{\mathrm{p},i}}{\Delta T_i}\right)\right] \qquad [12]$$

Note that Eq. [12] predicts that that mass at the peak rate of temperature change is $m_{0,i}\mathrm{e}^{-1}$ which is the same approximation derived by other authors[9]. Furthermore, the assumption of letting $\xi_i \to 0$ is equivalent to $RT_{\mathrm{p},i} \gg E_i$ which is the same assumption used to arrive at this approximation.

Reaction Peak Analysis

Equation [12] may be used in conjunction with TGA data to get estimates of the kinetic parameters. The approach developed in the following makes use of the fact that if the peak temperatures, $T_{\mathrm{p},i}$, are known from the data, it is possible to use derivatives of Eq. [12] to obtain estimates of ΔT_i and the total mass lost from the sample due to the reaction, Δm_i, from the data. Note that the total mass change associated with a reaction is

$$\Delta m_i \equiv m_{0,i}(1-\nu_i) \tag{13}$$

Taking the first three derivatives with respect to temperature of Eq. [12] results in

$$d_{1,i} \equiv (1-\nu_i)m_i' = \frac{\Delta m_i}{\Delta T_i} g_i \exp(g_i) \tag{14}$$

$$d_{2,i} \equiv (1-\nu_i)m_i'' = \frac{\Delta m_i}{\Delta T_i^2} g_i \exp(g_i)(g_i+1) \tag{15}$$

$$d_{3,i} \equiv (1-\nu_i)m_i''' = \frac{\Delta m_i}{\Delta T_i^3} g_i \exp(g_i)\left(g_i^2+3g_i+1\right) \tag{16}$$

where

$$g_i \equiv -\exp\left(\frac{T-T_{\mathrm{p},i}}{\Delta T_i}\right) \tag{17}$$

Note that the newly defined d-variables in Eqs. [14]-[16] represent the contribution of each component to the first three temperature derivatives of the total mass. Thus,

$$m' = \sum_i d_{1,i} \tag{18}$$

$$m'' = \sum_i d_{2,i} \tag{19}$$

$$m''' = \sum_i d_{3,i} \tag{20}$$

At the peak temperature, $g_i = -1$, and so Eqs. [14]-[16] yield

$$d_{1,i}\left(T_{\mathrm{p},i}\right) = -\frac{\Delta m_i}{\mathrm{e}\Delta T_i} \tag{21}$$

$$d_{2,i}\left(T_{\mathrm{p},i}\right) = 0 \tag{22}$$

$$d_{3,i}\left(T_{\mathrm{p},i}\right) = \frac{\Delta m_i}{\mathrm{e}\Delta T_i^3} \tag{23}$$

Equation [22] shows that the peak condition is in fact being satisfied. The solution of Eqs. [21] and [23] in gives

$$\Delta T_i = \sqrt{-\frac{d_{1,i}\left(T_{\mathrm{p},i}\right)}{d_{3,i}\left(T_{\mathrm{p},i}\right)}} \tag{24}$$

$$\Delta m_i = -\mathrm{e} d_{1,i}(T_{\mathrm{p},i})\Delta T_i \quad [25]$$

where, using Eqs. [18] and [20],

$$d_{1,i}(T_{\mathrm{p},i}) = m'(T_{\mathrm{p},i}) - \sum\nolimits_{j\neq i} d_{1,j}(T_{\mathrm{p},i}) \quad [26]$$

$$d_{3,i}(T_{\mathrm{p},i}) = m'''(T_{\mathrm{p},i}) - \sum\nolimits_{j\neq i} d_{3,j}(T_{\mathrm{p},i}) \quad [27]$$

In the following section, an algorithm is presented for using Eqs. [24]-[27] in conjunction with TGA data to obtain a set of kinetic parameters.

Description of Algorithm

In order to use Eqs. [24]-[27], it is necessary to have the temperature derivatives of the TGA data. That is, given the set of TGA data points for (T, m), what are the corresponding values of m', m'', and m''' at each temperature? It was found that the Savitzky-Golay filter[10] proved to be effective in estimating the derivatives of noisy TGA data. Application of the Savitzky-Golay filter requires two parameters: (1) the order of the polynomial fit and (2) the number of data points used in the fit. A quadratic fit was used for the first temperature derivative, a cubic fit for the second derivative, and a quartic fit was used for the third derivative data. The number of data points used in the fit was chosen to be enough to cover a temperature window of 10 K for the first temperature derivative, 20 K for the second derivative, and 40 K for the third derivative. These parameters were determined by trial and error, and future work will examine optimizing the choice of these parameters.

Once the first three derivatives of the TGA mass data were determined, it is necessary to determine the number of reactions. Clear reaction peaks correspond to points at which $m'' = 0$ and $m''' > 0$. All such peaks are easily obtained from the filtered temperature derivatives. Only peaks in which the mass loss rate was greater than 15% of the maximum peak mass loss rate were identified as distinct reactions. If two reactions occur over similar temperature ranges, it is often difficult to observe a distinct peak in the mass loss rate. However, in some cases the presence of a shoulder in the peak is evidence of a partially obscured reaction. Partially obscured reactions were found by locating points where m'' is small and $m''' = 0$.

The preceding paragraph presents two criteria for identifying reaction peaks. Each of these points corresponds to a temperature at which the peak occurs. So at this point in the algorithm, all that is stored is a set of N_{r} temperatures, $T_{\mathrm{p},i}$ for $i = 1, \ldots, N_r$. The next step is to determine the kinetic parameters for each of these reactions.

For the single reaction case, the total volatile mass lost from the reaction is equal to the total mass lost by the TGA sample, or

$$\Delta m_1 = \Delta m_{\mathrm{tot}} \equiv m_0 - m_{\mathrm{f}} \quad [28]$$

where m_0 and m_{f} are the initial and final masses of the sample. With only one reaction, Eq. [26] gives

$$d_{1,1}(T_{\mathrm{p},1}) = m'(T_{\mathrm{p},1}) \quad [29]$$

and so, upon substitution into and rearrangement of Eq. [25],

$$\Delta T_1 = -\frac{\Delta m_{\mathrm{tot}}}{\mathrm{e} m'(T_{\mathrm{p},1})} \quad [30]$$

If more than one peak is found, the process is complicated since the mass loss rate signals can overlap. An iterative approach has been developed in which an initial guess of all Δm_i and ΔT_i are used to compute Eqs. [26] and [27], and then the resultant values are used in Eqs. [24] and [25] to find updated values for these kinetic parameters. The process is repeated until convergence is achieved.

An important correction must be employed to insure that $\sum_i \Delta m_i = \Delta m_{\mathrm{tot}}$. Using Eqs. [24] and [25] for each reaction separately does not guaranty that this condition will be satisfied. In order, to identify a mass conserving mechanism an intermediate solution ΔT_i^* is found from Eq. [24]. The mass conserving peak widths would be those which satisfy

$$\Delta m_{\mathrm{tot}} = \sum_i -\mathrm{e} d_{1,i}\left(T_{\mathrm{p},i}\right)\Delta T_i \qquad [31]$$

The projection of the intermediate solution onto the space of solutions satisfying Eq. [31] is found by

$$\mathbf{\Delta T} = \mathbf{\Delta T}^* - \left(\frac{\mathbf{\Delta T}^* \cdot \mathbf{a} - \Delta m_{\mathrm{tot}}}{\mathbf{a} \cdot \mathbf{a}}\right)\mathbf{a} \qquad [32]$$

where $\mathbf{\Delta T}^*$ and $\mathbf{\Delta T}$ are simply the vectors formed from the temperature widths for the intermediate and mass conserving cases, and $\mathbf{a}$ is the vector whose elements are $a_i \equiv -\mathrm{e} d_{1,i}\left(T_{\mathrm{p},i}\right)$. The mass widths for an iteration are then found from the mass conserving temperature widths used in Eq. [25].

The entire algorithm for finding the kinetic parameters of TGA data indicating several reactions is summarized as follows:

1. Estimate reaction mass changes using $\Delta m_i = \Delta m_{\mathrm{tot}}/N_{\mathrm{r}}$ for each i.
2. Compute corresponding estimates of peak widths using $\Delta T_i = -\Delta m_i/\mathrm{e} m'\left(T_{\mathrm{p},i}\right)$ for each i.
3. Compute $d_{1,i}$ and $d_{3,i}$ for each i using the previously determined values for Δm_i and ΔT_i.
4. Find initial estimates ΔT_i^* for each i using Eq. [24].
5. Calculate mass conserving temperature widths using Eq. [32].
6. Calculate mass conserving reaction mass changes using Eq. [25].
7. Repeat steps 3 through 6 until Δm_i and ΔT_i converge.

It was found that even for the most complex scenarios considered that convergence was achieved after approximately 10 to 20 iterations making the algorithm extremely efficient. In the next two sections, the algorithm described in this section will be verified against manufactured data and validated against TGA data for several materials. In all cases, the algorithm requires less than one second of CPU time on a typical laptop computer to provide the complete set of kinetic parameters.

VERIFICATION

It is possible to verify the algorithm described in the preceding section by testing it against numerically generated TGA data based on an assumed kinetic model. In this process, TGA data is manufactured by simulating a solution of Eq. [4] using assumed parameter values. The algorithm was then applied to this manufactured data. The resultant calibrated kinetic parameters can be compared to the specified value, and predictions using the calibrated kinetic parameters can be compared to the manufactured data. In all cases, a heating rate of 10 K/min was used along with an initial sample mass of $m_0 = 1$.

One Reaction

Three single-reaction cases have been considered. Each of these three cases specify a peak reaction rate temperature at 650 K, and the sample was assumed to fully volatilize so that $m_{\mathrm{f}} = 0$ and $\Delta m = 1$.

In order to examine the effectiveness of the algorithm to handle a variety of data, three different characteristic peak widths were considered: $\Delta T = 10$ K, $\Delta T = 20$ K, and $\Delta T = 40$ K. The specified and calibrated parameters for these three cases are summarized in Tables 1-3. Plots of the TGA mass and mass loss rate for the three cases are provided in Figure 1. It is clear that the quality of the calibrated reaction decreases with increasing reaction width. This observation is likely a consequence of the fact that the fitting algorithm is based upon an approximate solution of the kinetic equations that assumes a small value of $\xi \equiv \Delta T/T_\mathrm{p}$. As the value of ΔT increases, so does the value of ξ, and thus the validity of the approximation decreases.

Table 1. Kinetic parameters for the single-reaction verification case with $\Delta T = 10$ K.

Kinetic Parameter	Specified Value	Calibrated Value
T_p (K)	650	649.4
ΔT (K)	10	9.99
ξ	0.01538	0.01539
$\ln[A\ (s^{-1})]$	60.91	60.90
E (kJ/kmol)	351.3×10^3	350×10^3

Table 2. Kinetic parameters for single-reaction verification case with $\Delta T = 20$ K.

Kinetic Parameter	Specified Value	Calibrated Value
T_p (K)	650	649.4
ΔT (K)	20	19.07
ξ	0.03077	0.02935
$\ln[A\ (s^{-1})]$	27.71	29.34
E (kJ/kmol)	175.6×10^3	184.1×10^3

Table 3. Kinetic parameters for single-reaction verification case with $\Delta T = 40$ K.

Kinetic Parameter	Specified Value	Calibrated Value
T_p (K)	650	649.4
ΔT (K)	40	36.
ξ	0.06154	0.05563
$\ln[A\ (s^{-1})]$	10.77	12.59
E (kJ/kmol)	87.8×10^3	97.1×10^3

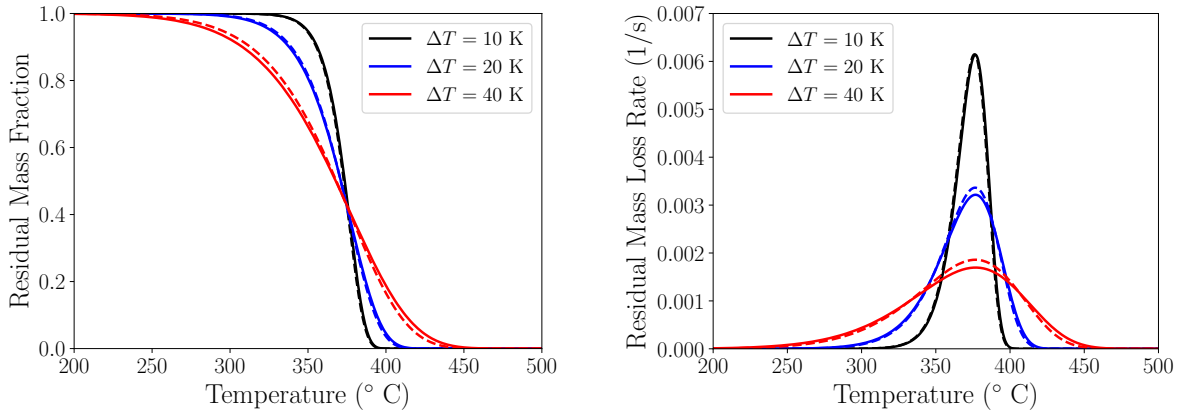

(a) (b)

Figure 1. Specified and calibrated TGA (a) normalized mass and (b) normalized mass loss rates for single-reaction verification cases. The solid lines represent the manufactured data and the dashed lines represent model predictions.

Two Reactions

Three two-reaction cases were also considered. For these cases, the effect of overlapping peaks was studied. For these scenarios, both reactions are assigned a characteristic peak width of 15 K. The normalized mass change associated with the first reaction is $\Delta m_1 = 0.5$, and that of the second reaction is $\Delta m_2 = 0.3$. In all cases, the midpoint between the two reaction peaks is 650 K. The difference between the cases is the distance between the peak temperatures. Three peak temperature differences were considered: 160 K, 80 K, and 40 K. The results of these three verification cases are provided in Figure 2. It is apparent that the algorithm captures the TGA signal well even as the peaks move close together. Although the plateau in the mass signal is overestimated, the mass loss rates are well captured—this is a consequence of the algorithm favoring mass loss rate matching over mass matching.

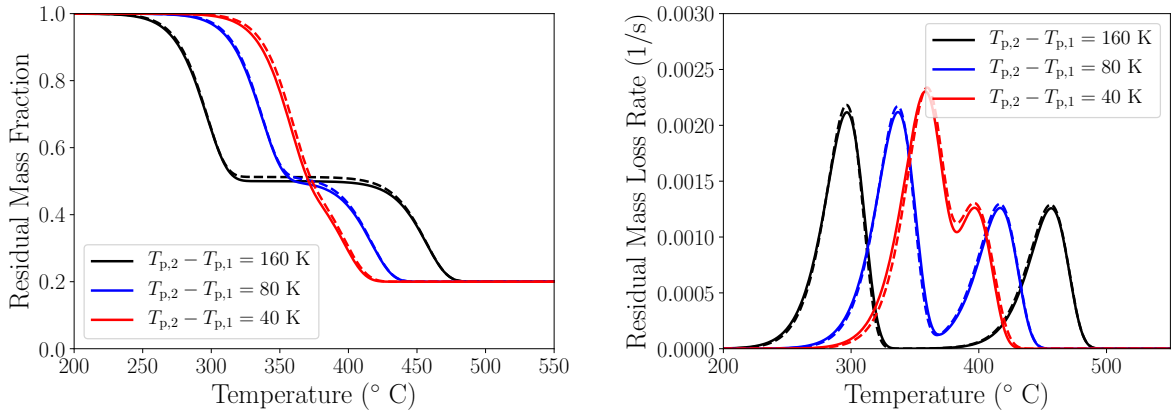

(a) (b)

Figure 2. Specified and calibrated TGA (a) normalized mass and (b) normalized mass loss rate for two-reaction verification cases. The solid lines represent the manufactured data and the dashed lines represent model predictions.

VALIDATION

The manufactured TGA data considered above represent an idealization of the complex processes actually occurring during the pyrolysis of real materials. It is therefore important to assess the validity of the fitting algorithm against real TGA data.

In this work, TGA experiments were conducted on three polymers: Polyamide 6,6 (Nylon 6,6), a flexible polyurethane (PU) foam, and polyvinyl chloride (PVC). These materials are widely used in construction, residential, and transportation applications, and, collectively, they present a diverse range of decomposition behaviors (e.g., single or multiple reaction peaks, discrete or overlapping reactions, and decomposition across a wide temperature range).

TGA experiments were conducted on these three materials in a Netzsch STA 449 F1 Jupiter. This apparatus continuously measures mass (using a microbalance with a 0.025 µg precision) and temperature (using an S-type thermocouple positioned directly beneath the sample crucible) of samples as they are heated through a well-defined temperature program in an anaerobic environment. A temperature calibration was conducted as per the manufacturer's recommendations[11] (using a set of 6 pure metals, with melting points between 156.6 and 961.8 °C) to provide a relation between measured and actual sample temperature. The calibration was performed using the same crucible type, heating rate, and gaseous environment as was used during thermal analysis experiments on the polymeric samples. All TGA experiments were conducted within three months of this calibration.

The temperature program used for TGA experiments included an initial isotherm at an elevated temperature (below 100 °C), during which time the chamber was continuously purged with nitrogen.

This ensured that the system was completely free of oxygen and that any residual moisture in samples was removed prior to dynamic heating and thermal decomposition. Following this conditioning period, samples were heated at a constant rate of 10 K/min up to 700 or 900 °C. Throughout this program, the test chamber was continuously purged with ultra-high purity (UHP) nitrogen at 50 mL/min. All tests were conducted in open alumina crucibles.

At the start of each day of testing, a baseline test was performed in which an empty alumina crucible was subjected to the same heating program as was used during the thermal analysis experiments. This baseline history (mass vs. temperature) was subtracted from the corresponding data obtained during experiments on the polymeric samples. All TGA measurement data presented in this work has been baseline-corrected in this manner. All samples were stored in a desiccator (in the presence of Drierite) for a minimum of 48 hours prior to testing. Immediately before testing, samples were removed from the desiccator, placed into alumina test crucibles, and weighed using a Mettler M3 analytical balance.

Polyamide 6,6 (Nylon 6,6)

Polyamide 6,6 (Nylon 6,6) samples were obtained from Goodfellow (Reference number AM323100) in the form of injection molded slabs, which were then cryogenically ground to obtain a powder for testing. For each test, between 4.5 and 5.5 mg of this powder was weighed and then pressed flat into the base of an alumina test crucible. The temperature program included a 20-minute-long isotherm at 27 °C followed by heating at a constant rate of 10 K/min to 900 °C. Three replicate tests were performed, and the average mass data was used by the algorithm to determine pyrolysis kinetics.

The calibrated kinetic parameters are listed in Table 4. Plots of the TGA data and the fit resulting from the calibrated parameters are provided in Figure 3 along with a gray area representing +/- two standard deviations of the mass data about the average mass. Although the initial onset temperature and the peak mass loss rate are slightly overpredicted, the predicted TGA agrees quite well with the experimental data.

Table 4. Calibrated kinetic parameters for Nylon 6,6.

Kinetic Parameter	Reaction 1
T_p (K)	716.3
ΔT (K)	22.11
Δm	0.9754
ξ	0.03087
$\ln[A\ (s^{-1})]$	27.50
E (kJ/kmol)	192.9×10^3

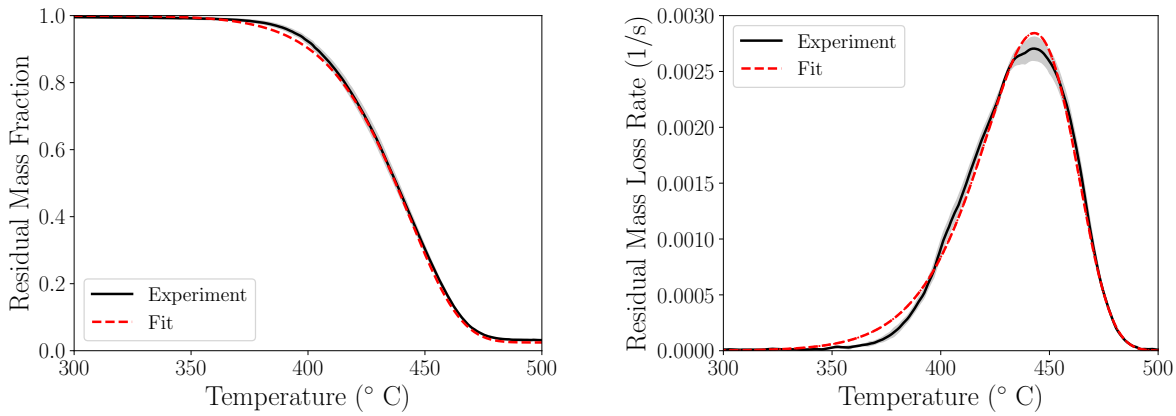

(a) (b)

Figure 3. Experimental and calibrated TGA (a) normalized mass and (b) normalized mass loss rate for Nylon 6,6. The gray area represents +/- two standard deviations about the average mass.

Flexible Polyurethane Foam

Polyurethane (PU) foam samples were produced by Innocor Foam Technologies to meet the specifications of a 'Standard Polyurethane Foam Substrate' described in ASTM-D3574-08[12]. This foam was purchased in the form of 8 cm thick slabs. Samples used for testing were cut from the center of these slabs into small, cylindrical pieces, between 3.0 and 5.0 mg in mass. These foam pieces were then compressed for a minimum of 72 hours before being pressed flat in the center of an alumina test crucible using a steel reshaping tool, just prior to testing. The temperature program included a 20-minute-long isotherm at 75 °C followed by heating at a constant rate of 10 K/min to 700 °C. Five replicate TGA tests were performed, and the average results were used to estimate kinetic parameters. The calibrated kinetic parameters are provided in Table 6. A plot of the experimental data along with the fit parameters is given in Figure 5. Again, the results predicted using the calibrated kinetic parameters agree quite well with the TGA data. In fact the predicted peak mass loss rates for both reactions are approximately equal to the experimental values.

Table 6. Calibrated kinetic parameters for PU foam.

Kinetic Parameter	Reaction 1	Reaction 2
T_p (K)	562.7	648.5
ΔT (K)	14.50	13.69
Δm	0.2511	0.7280
ξ	0.02577	0.02112
$\ln[A\ (s^{-1})]$	34.34	42.95
E (kJ/kmol)	181.5×10^3	255.3×10^3

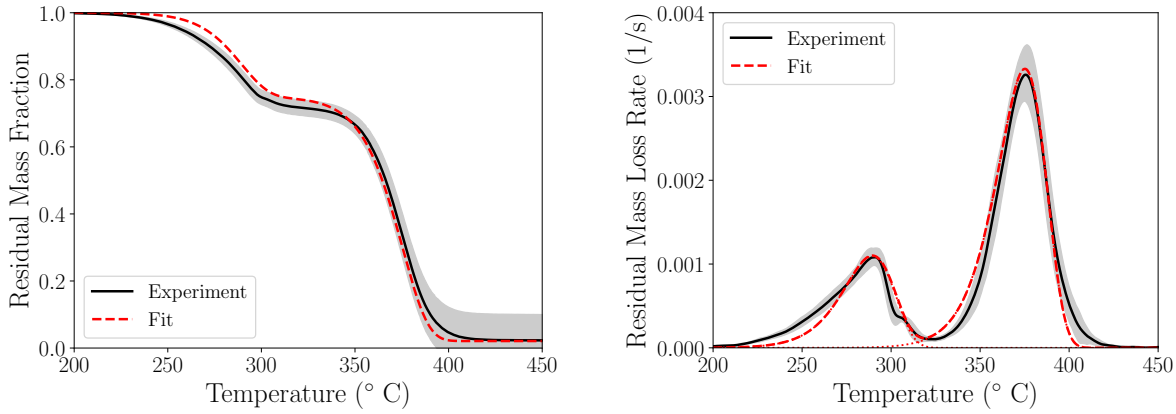

(a) (b)

Figure 5. Experimental and calibrated TGA (a) normalized mass and (b) normalized mass loss rate for PU foam. The gray area represents +/- two standard deviations about the average mass.

Polyvinyl Chloride

Polyvinyl chloride (PVC) samples were obtained from Interstate Plastics (manufactured by Vycom plastics: Type 1 PVC) in the form of 6 mm thick slabs. For each test, small, flat pieces between 4.5 and 5.5 mg in mass, were carefully cut from these slabs and placed in the center of an alumina test crucible. The temperature program included a 30-minute-long isotherm at 40 °C followed by heating at a constant rate of 10 K/min to 700 °C. Six replicates were performed, and the average TGA signal was used to calibrate the kinetic parameters. The algorithm predicts a three-reaction mechanism, and the calibrated kinetic parameters are tabulated in Table 5. The data and corresponding fits are provided in Figure 4. It is apparent that the fit is not as good as was obtained for the other two materials. This can be attributed to the relative noisiness of the experimental data along with the fact

that the first two reactions are relatively close to one another. However, the peak mass loss rates for all three reactions is very well captured by the calibrated kinetic model. The adequacy of this, or any fit, ultimately depends on the ability of the calibrated parameters to make accurate predictions of burning rate and flame spread in fire models. Such a study is beyond the scope of this paper.

Table 5. Calibrated kinetic parameters for PVC.

Kinetic Parameter	Reaction 1	Reaction 2	Reaction 3
T_p (K)	568.5	731.7	588.1
ΔT (K)	12.15	22.39	9.62
Δm	0.4200	0.2238	0.1999
ξ	0.02138	0.03060	0.01636
$\ln[A\ (s^{-1})]$	42.49	27.78	57.06
E (kJ/kmol)	221.1×10^3	198.8×10^3	298.8×10^3

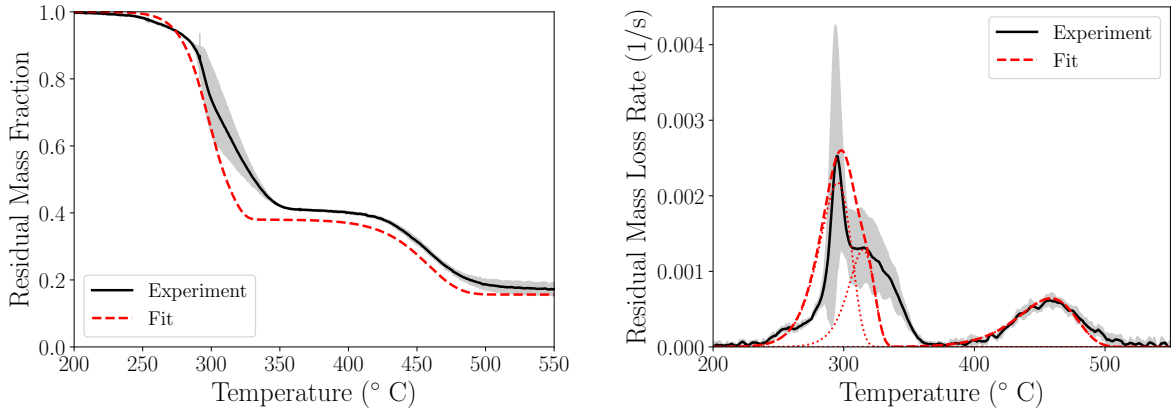

(a) (b)

Figure 4. Experimental and calibrated TGA (a) normalized mass and (b) normalized mass loss rate for PVC. The gray area represents +/- two standard deviations about the average mass.

Further validation of the algorithm has been performed for 11 different vegetative fuels[13]. These vegetative fuels typically exhibited 2-3 reaction peaks within close proximity and with considerable noise in the data. As can be confirmed in the reference, the automated fitting algorithm described in this paper performed well even in these more challenging scenarios.

CONCLUSIONS

A novel methodology has been presented for finding the kinetic parameters of pyrolysis from TGA data. The advantages of this algorithm are that (1) it is fully-automated requiring no interaction from the user, (2) it is computationally efficient in providing the kinetic parameters in less than one second, and (3) it has been verified and validated. The need for such a methodology is driven by a demand for material properties needed as inputs for fire models of flame spread.

Verification was performed by applying the algorithm to manufactured data for several one and two reaction pyrolysis mechanisms. As expected by the underlying theory, it was found that the algorithm performed better for narrower reactions. Additionally, slightly better fits were obtained for well-separated reaction peaks. For the two-reaction scenarios, it was found that the algorithm can sometimes fail to exactly predict mass plateaus between reactions. This is a consequence of the fact that the methodology focuses primarily on capturing the mass loss rate as opposed to the sample mass. A focus on the mass loss rate is justified since flammability is governed by the rate at which combustible volatiles are generated rather than the current amount of mass remaining in the sample. The results of the different verification cases demonstrate that even in situations in which the mass signal is not perfectly captured, the mass loss rate is quite accurate.

Three different materials were used to validate the algorithm: Nylon 66, PVC, and flexible polyurethane foam. All TGA tests for these three materials were performed at a heating rate of 10 K/min in a nitrogen environment with the samples placed in an alumina crucible. These cases proved to be a rigorous test of the algorithm since the materials varied in the number of reactions predicted as well as the noise in the underlying data. Kinetic parameters for all three of these materials were determined using the automated algorithm, and the resultant model predictions agreed with the data nicely.

Although the algorithm has been verified and validated to some extent, more validation is always desirable in order to find the limits of applicability of the algorithm. The results presented in this paper are quite promising, but it would be desirable to make better fits for broader peaked reactions as well as for overlapping reactions that occur at very similar temperatures. Furthermore, as was seen in the validation cases, different materials can produce different amounts of noise in the raw TGA data. It would therefore be helpful to make the algorithm more robust against varying degrees of noise. These improvements are primarily related to the very first step in the algorithm which uses the Savitzky-Golay filter to smooth the data and find sufficiently smoothed derivatives. There are several parameters involved in this process that need to be optimized by further study.

Finally, the true test of the effectiveness of this novel methodology lies in its effectiveness at providing parameters that accurately predict burning rate and flame spread in fire models such as FDS. Future work will therefore involve developing similar procedures to use other microscale data such as differential scanning calorimeter (DSC) and microscale combustion calorietery (MCC) to estimate the other parameters needed in fire models. Once a more complete program of automation is achieved, it will be possible to validate the procedures by comparing fire model results with experimental flame spread data of real materials. Such a process will take significant effort, but the present paper provides a critical first step in this direction.

REFERENCES

1. McGrattan, K.B., et al., “Fire Dynamics Simulator, Volume 1: Mathematical Model,” NISTIR, Special Publication 1018-1 Sixth Edition. National Institute of Standards and Technology, Gaithersburg, MD (2019).
2. Lautenberger, C., Fernanez-Pello, C., “Generalized pyrolysis model for combustible solids,” Fire Safety Journal, 44:819–839 (2009).
3. Stoliarov, S.I., Lyon, R.E, “Thermo-kinetic model of burning,” Technical Report DOT/FAA/AR-TN08/17, FAA (2008).
4. Stoliarov S.I., Li J., “Parameterization and Validation of Pyrolysis Models for Polymeric Materials; Fire Technology, 52:79-91 (2016).
5. McGrattan, K.B., et al., “Fire Dynamics Simulator: Technical Reference Guide, Volume 3: Validation,” NISTIR, Special Publication 1018-1 Sixth Edition. National Institute of Standards and Technology, Gaithersburg, MD (2019).
6. Brown, A., et al., “Proceedings of the first workshop organized by the IAFSS Working Group on Measurement and Computation of Fire Phenomena (MaCFP),” Fire Safety Journal, 101:1-17 (2018).
7. Bruns, M.C., Koo, J.H., Ezekoye, O.A. “Population-based models of thermoplastic degradation: using optimization to determine model parameters,” Polymer Degradation and Stability, 94(6):1013–1022 (2009).
8. Bruns, M.C., “Inferring and Propagating Kinetic Parameter Uncertainty for Condensed Phase Burning Models,” Fire Technology, 52(1):93-120 (2016).
9. McGrattan, K.B., et al., “Fire Dynamics Simulator: Technical Reference Guide, User’s Guide,” NISTIR, Special Publication 1019 Sixth Edition. National Institute of Standards and Technology, Gaithersburg, MD (2019).
10. Savitzky, A., Golay, M.J.E. "Smoothing and Differentiation of Data by Simplified Least Squares Procedures," Analytical Chemistry, 36 (8):1627–39 (1964).
11. NETZSCH, “Software Manual (STA 449 F1 & F3) Temperature and Sensitivity Calibration,” Wittelsbacherstrasse 42, 95100 Selb, Germany: NETZSCH Gerätebau GmbH (2012).

12. ASTM D3574-08, “Standard Test Methods for Flexible Cellular Materials—Slab, Bonded, and Molded Urethane Foams,” ASTM International: West Conshohocken, PA, USA (2008).
13. Leventon, I.T., Bruns, M.C., “Thermal Decomposition of Vegetative Fuels,” 15th International Conference and Exhibition on Fire Science and Engineering (Interflam), London, UK (2019).